A REVIEW OF APPROXIMATE METHODS IN SUBSONIC COMPRESSIBLE FLOW

By Carl Kaplan

Langley Aeronautical Laboratory

INTRODUCTION

The purpose of this paper is to review several methods developed in recent years for the calculation of the flow of a compressible fluid past a prescribed body. These methods have evolved largely because of the inherent difficulty of handling the nonlinear partial differential equations which govern the flow of a compressible fluid. In the discussion of these methods several points of mathematical interest will be noted for possible future investigations.

The study of fluid-flow phenomena at high speeds requires the consideration of compressibility and therefore of the thermodynamics of the fluid. For a real fluid, this would be a practically impossible problem. In this review, therefore, the fluid is considered to be a perfect one with vanishingly small viscosity and heat conductivity. The discussion is confined, moreover, mainly to irrotational flow in two dimensions with a subsonic undisturbed flow.

It is assumed that the fluid is a perfect gas so that the equation of state is

$$p = RT\rho \tag{1}$$

The equations of motion for the fluid are

$$\left.\begin{aligned} u\frac{\partial u}{\partial x} + v\frac{\partial u}{\partial y} &= -\frac{1}{\rho}\frac{\partial p}{\partial x} \\ u\frac{\partial v}{\partial x} + v\frac{\partial v}{\partial y} &= -\frac{1}{\rho}\frac{\partial p}{\partial y} \end{aligned}\right\} \tag{2}$$

and the equation of continuity is

$$\frac{\partial \rho u}{\partial x} + \frac{\partial \rho v}{\partial y} = 0 \tag{3}$$

where

x, y rectangular coordinates in plane of flow

u, v components of velocity vector

p pressure in fluid

ρ density of fluid

T temperature of fluid

R gas constant

With the assumption of vanishingly small viscosity and heat conductivity, the behavior of the fluid in motion is closely isentropic so that p and ρ are related by the equation

$$p = k\rho^{\gamma} \tag{4}$$

where γ is the ratio of specific heats at constant pressure and constant volume and k is an arbitrary constant. The Bernoulli integral of the equations of motion (2) then becomes

$$c^2 = c_{\infty}^2\left[1 - \frac{\gamma - 1}{2} M_{\infty}^2\left(\frac{q^2}{U^2} - 1\right)\right] \tag{5}$$

where

c local velocity of sound $\left(c = \sqrt{\frac{dp}{d\rho}}\left(= \sqrt{\gamma\frac{p}{\rho}}\right)\right)$

c_{∞} velocity of sound in undisturbed stream

q magnitude of fluid velocity

U velocity of undisturbed stream

M_{∞} Mach number in undisturbed stream $\left(\frac{U}{c_{\infty}}\right)$

With the assumption of irrotationality, a velocity potential ϕ can be introduced, where

$$\left.\begin{aligned} u &= \frac{\partial\phi}{\partial x} \\ v &= \frac{\partial\phi}{\partial y} \end{aligned}\right\} \tag{6}$$

Then the elimination of ρ from equations (2) and (3) yields the fundamental differential equation governing the flow; namely,

$$\left(c^2 - u^2\right)\frac{\partial^2\phi}{\partial x^2} - 2uv\,\frac{\partial^2\phi}{\partial x\partial y} + \left(c^2 - v^2\right)\frac{\partial^2\phi}{\partial y^2} = 0 \tag{7}$$

a nonlinear, second-order partial differential equation.

METHODS OF APPROXIMATE SOLUTION

The rigorous treatment of the fundamental differential equation (7) for nonlinearized flow past closed shapes with general boundary conditions has up to the present time proved to be impossible. In place of rigorous analytical solutions it is necessary to be satisfied in general with approximation methods essentially based on the linearization of equation (7). The mathematical difficulties are considerably greater for subsonic flow (elliptic potential equation) than for supersonic flow (hyperbolic potential equation), for which the theory of characteristics leads to very simple approximation methods. Three of the methods which have been utilized for subsonic flow will be described in the remainder of this paper.

Method of Expansion in Powers of the Mach Number

In the Rayleigh-Janzen method the velocity potential ϕ is expanded in a series of powers of M_∞^2,

$$\phi = \phi_0 + M_\infty^2\phi_1 + M_\infty^4\phi_2 + \ldots \tag{8}$$

where ϕ_0 is the velocity potential of the incompressible fluid flow and thus satisfies the boundary conditions. The appropriate form of the differential equation for ϕ is obtained by rewriting equation (7) with the aid of equation (5). Thus

$$\left[1 - \frac{\gamma - 1}{2} M_\infty^2\left(\frac{q^2}{U^2} - 1\right)\right]\Delta\phi = \frac{1}{2} M_\infty^2\left[\frac{\partial\phi}{\partial x}\frac{\partial}{\partial x}\left(\frac{q^2}{U^2}\right) + \frac{\partial\phi}{\partial y}\frac{\partial}{\partial y}\left(\frac{q^2}{U^2}\right)\right] \tag{9}$$

where the symbol Δ denotes the Laplacian operator

$$\frac{\partial^2}{\partial x^2} + \frac{\partial^2}{\partial y^2}$$

The expression for ϕ from equation (8) is then inserted in equation (9) and coefficients of corresponding powers of M_∞ on either side are equated, yielding successively the equations for ϕ_0, ϕ_1, ... Thus

$$\left.\begin{aligned} \Delta\phi_0 &= 0 \\ \Delta\phi_1 &= \frac{1}{2}\left[\frac{\partial\phi_0}{\partial x}\frac{\partial}{\partial x}\left(\frac{q_0^2}{U^2}\right) + \frac{\partial\phi_0}{\partial y}\frac{\partial}{\partial y}\left(\frac{q_0^2}{U^2}\right)\right] \\ &\cdot\ \cdot\ \cdot\ \cdot\ \cdot \end{aligned}\right\} \qquad (10)$$

where q_0 is the magnitude of the incompressible flow velocity.

Rayleigh (reference 1) and Janzen (reference 2) were the first to consider the second of equations (10) and gave a series solution for ϕ_1 in the case of the flow past a circular cylinder. Later, Poggi (reference 3) introduced a method that consists essentially in considering the compressible fluid to be an incompressible fluid with a continuous distribution of sinks and sources in the entire region external to the solid boundary. According to Poggi, the right-hand sides of equations (10) represent successive terms in an infinite series giving this sink-source distribution. Poggi and later Kaplan (references 4 and 5) and Imai (reference 6) obtained the solution from this point of view for the flow past such shapes as a circular cylinder, an elliptic cylinder, and a Joukowski profile with angle of attack and circulation. The calculations proved to be extremely laborious, involving a large number of double integrals. In order to ease the labor involved in the original Poggi method, Imai and Aihara (reference 7) and Kaplan (reference 8) developed elegant and useful methods which utilized the theory of functions of a complex variable. The one to be described in this review is that due to Kaplan, which makes use of the calculus of residues. Thus, if new independent variables $z = x + iy$ and $\overline{z} = x - iy$ are introduced, the expression for the strength of the sink-source distribution obtained from the right-hand side of the second of equations (10) may be written as follows:

$$-\frac{1}{4\pi U^2}\left(w_0^2\frac{d\overline{w}_0}{d\overline{z}} + \overline{w}_0^2\frac{dw_0}{dz}\right)dx\ dy \qquad (11)$$

where w_o and $\bar{w}_o$ are, respectively, the complex and conjugate complex velocities of the incompressible fluid past the prescribed shape; that is, $w_o = -u + iv$ and $\bar{w}_o = -u - iv$ and these are, respectively, functions of z and $\bar{z}$ only, since they are obtained from solutions of Laplace's equation. Now, the expression, equation (11), involves non-analytic functions of z and $\bar{z}$. In order, however, to utilize the methods of the calculus of residues, functions of only a single complex variable must appear. For this purpose the plane z of the obstacle is represented conformally on the plane Z of the corresponding circle. Since the strengths of the sink-source distribution of corresponding elements of the two planes are equal, the expression for the strength of the sink-source distribution of an element of the plane Z is

$$-\frac{1}{4\pi U^2}\left[W_o{}^2 \frac{dZ}{dz} \frac{d}{d\bar{Z}}\left(\bar{W}_o \frac{d\bar{Z}}{dz}\right) + \bar{W}_o{}^2 \frac{d\bar{Z}}{d\bar{z}} \frac{d}{dZ}\left(W_o \frac{dZ}{dz}\right)\right] dX\, dY \qquad (12)$$

where W_o and $\bar{W}_o$ are, respectively, the complex and conjugate complex velocities of the incompressible fluid past the circular profile in the plane Z.

It is a simple matter to obtain an expression for the complex velocity W_1 induced at any point Z_p external to the circular boundary by a sink-source distribution originating in the physical plane z and at the same time to preserve the boundary conditions of zero normal velocity at the circular boundary and zero induced velocity at infinity. The essential fact to remember is that corresponding to a unit external source there is a unit source at the inverse point with respect to the circle and a unit sink at the center of the circle. The actual velocity w_1 of the fluid in the physical plane z is related to the velocity W_1 at the corresponding point in the plane Z of the circle by the equation

$$w_1 = W_1 \frac{dZ}{dz} \qquad (13)$$

The expression for W_1 consists of double integrals whose integrands are non-analytic functions of Z and $\bar{Z}$. The double integrations over the entire region external to the circular boundary can be replaced by line integrals involving functions of Z and $\bar{Z}$ only by the use of Stokes' theorem for the plane. Thus, it can be shown that if $F(Z,\bar{Z})$

is a function of Z and $\bar{Z}$, continuous and differentiable in the area S enclosed by the contour C, then

$$\left.\begin{aligned} \int_C F(Z,\bar{Z})d\bar{Z} &= -2i\int_S \frac{\partial F}{\partial Z}\,dS \\ \int_C F(Z,\bar{Z})dZ &= 2i\int_S \frac{\partial F}{\partial \bar{Z}}\,dS \end{aligned}\right\} \qquad (14)$$

The line integrals, in the present case, are taken around the circular boundary corresponding to the actual profile in the z-plane, around an infinitely small circle surrounding the point at which W_1 is to be evaluated, and around an infinitely large circle concentric with the internal circular boundary. The important point to note is that, since all the contours involved in the line integrations are circular, the integrands can be made analytic in Z or $\bar{Z}$, since on a circular boundary $Z\bar{Z}$ = Constant. It then follows that the line integrals can be evaluated by means of Cauchy's theorem on residues. This theorem states that, if a function is analytic on a contour C and throughout its interior except at a number of poles inside the contour, then

$$\left.\begin{aligned} \int_C G(Z)dZ &= 2\pi iM \\ \int_C H(\bar{Z})d\bar{Z} &= -2\pi iN \end{aligned}\right\} \qquad (15)$$

where M and N are, respectively, the sum of the residues at those poles which lie within the contour C.

The device of introducing z and $\bar{z}$ as independent variables, then utilizing the conformal mapping of the plane of the obstacle into the plane of a circle, and finally replacing the double integrals by line integrals thus enables one to evaluate by the method of residues the first effect of compressibility on the velocity of the fluid past an arbitrary shape. The point of interest to an applied mathematician is that here is a method whereby a Poisson equation involving rather complicated boundary conditions can be solved with the aid of analytic functions of a single complex variable. The subject is certainly worthy of further investigation.

Method of Small Perturbations

Whereas the preceding treatment started with the incompressible flow, the Prandtl–Busemann or Ackeret method starts with the undisturbed flow. It is applicable to the flow past thin shapes placed in a uniform stream, in which the changes in the velocity of the fluid as it passes over the body are small compared with the main stream velocity. The velocity potential is developed in a power series of a perturbation parameter ϵ (which may be the thickness coefficient, the camber coefficient, or the angle of attack) in which the first term is the velocity potential of the undisturbed stream $\phi_0 = Ux$. Thus, it is assumed that

$$\phi = Ux + \epsilon\phi_1 + \epsilon^2\phi_2 + \epsilon^3\phi_3 + \dots \tag{16}$$

where the ϕ_n are functions of x, y and of M_∞ and show successively the effects of compressibility on the flow.

The assumed series, equation (16), is inserted into the combined nonlinear equations (7) and (5) and the successive linear equations for ϕ_1, ϕ_2, ... can then be obtained by equating the coefficients of successive powers of the perturbation parameter ϵ. The first two equations obtained by this procedure are

$$\left.\begin{aligned} &\left(1 - M_\infty^2\right)\frac{\partial^2\phi_1}{\partial x^2} + \frac{\partial^2\phi_1}{\partial y^2} = 0 \\ &\left(1 - M_\infty^2\right)\frac{\partial^2\phi_2}{\partial x^2} + \frac{\partial^2\phi_2}{\partial y^2} = M_\infty^2\left[(\gamma + 1)\frac{\partial\phi_1}{\partial x}\frac{\partial^2\phi_1}{\partial x^2}\right. \\ &\qquad\left. + (\gamma - 1)\frac{\partial\phi_1}{\partial x}\frac{\partial^2\phi_1}{\partial y^2} + 2\frac{\partial\phi_1}{\partial y}\frac{\partial^2\phi_1}{\partial x\partial y}\right] \end{aligned}\right\} \tag{17}$$

These differential equations may be put into more familiar forms by introducing a new set of independent variables X and Y by means of the following affine transformation:

$$\left. \begin{aligned} X &= x \\ Y &= \sqrt{1 - M_\infty^{\ 2}}\ y \end{aligned} \right\} \tag{18}$$

Thus, for $M < 1$, the first of equations (17) is transformed into a Laplace equation and the succeeding equations for $\phi_2, \phi_3, \ldots$ into Poisson equations in which the right-hand sides are known functions of X and Y determined from the preceding approximations. The solution of the first of equations (17) yields the well-known Prandtl-Glauert rule, whereas the solutions of the succeeding Poisson equations provide higher approximations to the flow of the compressible fluid and thus will apply for larger departures from the undisturbed uniform flow.

The general procedure followed in solving equations (17) is simple in principle. The first step is to obtain an expression for the velocity potential of the incompressible flow past the prescribed boundary in the form of a power series in the perturbation parameter ϵ. Then the solution for the first approximation ϕ_1 to the compressible flow is easily obtained by analogy from the coefficient of the first power of ϵ. The higher approximations $\phi_2, \phi_3, \ldots$ are obtained by solving the corresponding Poisson equations, at the same time satisfying the boundary conditions to the same power of the perturbation parameter ϵ as is involved in the expression for the velocity potential ϕ.

Thus, consider the first approximation ϕ_1; if

$$\phi = UX + \epsilon\phi_1 (X,Y) \tag{19}$$

represents the incompressible flow past a body, then to the same order of approximation,

$$\left. \begin{aligned} \phi &= Ux + \frac{\epsilon}{\beta}\,\phi_1\ (x,\beta y) \\ \beta &= \sqrt{1 - M_\infty^{\ 2}} \end{aligned} \right\} \tag{20}$$

represents the compressible flow past the same body.

Now, if q_c and q_i denote the magnitudes of the velocity at the surface of the prescribed shape for the compressible and incompressible flows, respectively, then to the first power of ϵ the perturbation term (evaluated at the boundary) is the same for the two cases. The result is a relation between q_c and q_i, independent of the particular shape prescribed; namely,

$$\frac{q_c}{q_i} = \frac{1}{\beta} - \left(\frac{1}{\beta} - 1\right)\frac{U}{q_i} \tag{21}$$

Equation (21) represents the so-called velocity correction formula for the Prandtl-Glauert approximation.

This method of iteration by powers of a perturbation parameter ϵ has been applied to a family of symmetrical shapes (bumps, reference 9) and to a family of circular arcs (reference 10), specifically chosen because they possess no stagnation points and hence satisfy the primary assumption of the method; namely, small disturbances to the oncoming uniform stream. The iterations included the third power of the thickness coefficient in the case of the family of symmetrical shapes and the third power of the camber coefficient in the case of the family of circular arcs. It is important to remark that, although extensive use was made of the affine transformation, equation (18), the boundary conditions were always satisfied in the plane of the actual profiles.

In general, the affine transformation, equation (18), introduces a distortion of the solid boundary which depends on the stream Mach number. This distortion, therefore, in general precludes the use of analytic function methods. In the case of a family of elliptic profiles, however, the affine transformation produces another family of elliptic profiles. Since one ellipse differs from another only with respect to the thickness coefficient, it is possible to treat the problem in the plane of the circle corresponding to the plane of the affine ellipse. For this purpose it is simpler, from the point of view of satisfying the boundary conditions, to treat the equations for the stream function corresponding to equations (17). The results obtained in the plane of the circle, making extensive and elegant use of functions of a single complex variable, are easily transferred into the physical plane of the actual elliptic profile. Such calculations have been performed for the case of an elliptic cylinder with both angle of attack and circulation (references 11, 12, and 13). Typical of the results obtained is the following formula relating the lift on an elliptic cylinder in a compressible and an incompressible flow:

$$\frac{L_c}{L_i} = \frac{1}{\beta} + \frac{1}{2}\left(1 - e^{-2\lambda}\right)\left[\frac{1-\beta}{\beta^2} + \frac{1}{4}(\gamma + 1)\left(\frac{1-\beta^2}{\beta^2}\right)^2\right] \tag{22}$$

where

$\beta = \sqrt{1 - M_\infty^2}$

γ ratio of specific heats at constant pressure and at constant volume

e^λ proportional to radius of circle conformal to actual ellipse in physical plane

Equation (22) is an extension of the well-known Prandtl-Glauert rule to thicker profiles and is applicable not only to an ellipse but to an arbitrary symmetrical shape.

The method just described, utilizing the powerful tool of complex-function theory, could be extended to arbitrary profiles if the answer to the purely mathematical question of the effect of an affine transformation on the coefficients of the conformal mapping function to a circle were known. Another interesting and important problem is the convergence of the precedure herein described. Calculations indicate that the power-series development of the velocity potential or of the stream function in powers of a perturbation parameter may converge somewhat beyond the critical stream Mach number, but a rigorous discussion of this question has yet to be given.

In order to show the entent to which the methods of Rayleigh and Janzen and of Prandtl and Busemann apply to practical airfoils, figure 1 has been prepared. The stream Mach number M_∞ is the abscissa and the thickness coefficient t is the ordinate. The critical stream Mach number curve bounds the subsonic flows. The method of Rayleigh and Janzen proceeds in the direction of increasing stream Mach number and yields at each stage exact information with regard to the geometry of the profile. The vertical lines separate the regions of the second and third approximations, the line $M_\infty = 0$ being the incompressible solution. It is clear that many approximations would be necessary to penetrate into the region of interest to aeronautics, that is, between $t = 5$ percent and $t = 15$ percent.

The method based on the Prandtl-Glauert linearized result proceeds in the direction of increasing thickness and yields at each stage exact information with regard to the stream Mach number. The horizontal lines separate the regions in which the Prandtl-Glauert correction holds and the first additional step. This figure shows clearly that, already by a first-step improvement of the Prandtl-Glauert result, significant results are obtained in the region of interest to aeronautics whereas similar success by means of the Rayleigh-Janzen method would entail a prohibitive amount of labor.

Method of the Hodograph

It is clear from the discussion in the foregoing sections that both the Rayleigh–Janzen and the Prandtl–Busemann procedures become rather laborious after one or two steps; moreover, such calculations must be repeated from the beginning for each prescribed solid boundary. Consequently, many attempts have been made to set up a correspondence between incompressible flows and compressible flows of the nature of correction factors. Among the better known results of such attempts are the Prandtl–Glauert (reference 14), von Kármán–Tsien (reference 15), Temple–Yarwood (reference 16), and Garrick–Kaplan (references 17 and 18) velocity correction formulas – all of which depend only on the incompressible fluid velocity and the stream Mach number.

Before proceeding with the discussion of velocity correction formulas, a rather instructive comparison is given of the compressibility effect on the maximum velocity of a series of bumps and circular arcs. The thickness coefficients of the bumps and the camber coefficients of the corresponding circular arcs were so chosen that the incompressible speeds were the same. Table I shows the results calculated by the Prandtl–Busemann iteration method – the calculations included the third power of the thickness and camber coefficients. For moderate values of thickness and camber the differences are seen to be negligible over most of the subsonic range. These calculations indicate that, to a very good approximation, the effect of compressibility in the subsonic range depends essentially only on the incompressible fluid velocity and on the undisturbed stream Mach number and is largely independent of the particular solid boundary treated. This result substantiates the feasibility of velocity correction formulas in the subsonic range of speeds.

From the nature of velocity correction formulas it would seem that the hodograph plane variables are the appropriate ones to consider. The hodograph variables are q, the magnitude of the fluid velocity, and θ, the angle included by the velocity vector and the positive direction of the x–axis. Corresponding to q^k in the incompressible case, there appear functions $P_k(q)$ and $Q_k(q)$ in the compressible case, where

$$\left.\begin{aligned} \frac{1}{k}\log Q_k &= \log q + f_k(\tau) \\ \frac{1}{k}\log P_k &= \log q + g_k(\tau) \end{aligned}\right\} \qquad (23)$$

The functions $P_k(q)$ and $Q_k(q)$ are associated, respectively, with the velocity potential and the stream function in the compressible case; the functions $f_k(\tau)$ and $g_k(\tau)$ are related to the particular solutions of Chaplygin's basic differential equation of the hypergeometric type for compressible flow. The variable τ is a dimensionless speed variable defined as follows:

$$\tau = \frac{q^2}{q_{max}^2} = \frac{M^2}{\frac{2}{\gamma - 1} + M^2}$$

where q_{max} is the maximum fluid velocity corresponding to expansion into a vacuum. Figure 2 shows the graphs of several of the (hypergeometric) functions f_k and g_k for positive values of k with the Mach number as abscissa. The value of γ chosen was 1.4 for air. Note that, as the subscript k is increased, both sets of functions approach the single function $f_\infty = g_\infty = h(\tau)$ defined between the limits $M = 0$ and $M = 1$. According to equations (23) then, as $k \rightarrow \infty$,

$$P_k \approx Q_k \approx \left[q e^{h(\tau)}\right]^k \tag{24}$$

The nature of the correspondence between incompressible and compressible flow is assumed to be such that

$$\left.\begin{aligned} \phi_i(q_i, \theta) &= \phi_c\left[q_c e^{f_k(\tau)}, \theta\right] \\ \psi_i(q_i, \theta) &= \psi_c\left[q_c e^{g_k(\tau)}, \theta\right] \end{aligned}\right\} \tag{25}$$

where ψ denotes the stream function and the subscripts i and c refer, respectively, to incompressible and compressible flow. In order to obtain a correspondence of velocities, it is necessary that also for the compressible case the speed variable be the same for both the velocity potential and the stream function. The function $h(\tau)$ separating, as it does, the two sets of functions $f_k(\tau)$ and $g_k(\tau)$ is peculiarly suited for this purpose. Thus, the correspondence of velocities in the incompressible and the compressible case is given by

$$q_i = q_c e^{h(\tau)} \tag{26}$$

Equation (26) constitutes the geometric-mean type of velocity correction formula introduced in reference 16 and is limited to the subsonic range $0 \leq M \leq 1$. As already noted, for positive values of k, $h(\tau)$ lies between $f_k(\tau)$ and $g_k(\tau)$ in magnitude. Moreover, the deviation of $e^{h(\tau)}$ from $e^{f_k(\tau)}$ and $e^{g_k(\tau)}$ is quite small in the entire subsonic range.

The geometric-mean type of velocity correction formula contains the results of Chaplygin, von Kármán and Tsien, Temple and Yarwood, and, in the limiting case of small disturbances to the main flow, the exact Prandtl-Glauert rule. For example, the von Kármán-Tsien velocity correction formula is obtained from the geometric-mean type of approximation by taking $\gamma = -1$. The geometric-mean type of velocity correction formula just described seems to be the most logical one from a mathematical point of view. It is interesting to note, however, that the choice of $\gamma = -1$, yielding the Kármán-Tsien formula, appears to cancel the effect of boundary distortion inherent in the correspondence equations (25). This fortuitous circumstance, together with the simplicity of the calculations involved, makes it very useful for most purposes. Figure 3 illustrates in general the usefulness of velocity correction formulas and in particular the one given by von Kármán and Tsien. The solid curves show the variation of the maximum pressure coefficient with the stream Mach number for several members of a family of symmetrical profiles (bumps) calculated by means of the Prandtl-Busemann iteration in powers of the thickness coefficient (reference 9). The small circles show the results obtained by means of the von Kármán-Tsien velocity correction formula. The agreement between the two methods over such a wide range in thickness coefficients and stream Mach numbers is remarkable. Indeed, the development of velocity correction formulas and their use in the prediction of compressibility effects should be considered as an outstanding achievement of theoretical aerodynamics. For, consider that the problem of compressible flow involves a nonlinear differential equation for which very little mathematical treatment is available; nevertheless, with the aid of a few simple ideas and very little labor the essential results can be obtained by means of velocity correction formulas. One must be cautioned, however, that their use is limited to the subsonic range and must not be extended into the transonic or mixed subsonic and supersonic range of speeds.

REFERENCES

Method of Expansion in Powers of the Mach Number

1. Rayleigh, (Lord): On the Flow of Compressible Fluid past an Obstacle. Phil. Mag., ser. 6, vol. 32, no. 187, July 1916, pp. 1-6.
2. Janzen, O.: Beitrag zu einer Theorie der stationären Strömung kompressibler Flüssigkeiten. Phys. Zeitschr. Jahrg. 14, Nr. 14, July 15, 1913, pp. 639-643.
3. Poggi, Lorenzo: Campo di velocità in una corrente piana di fluido compressibile. L'Aerotecnica, vol. XII, fasc. 12, Dec. 1932, pp. 1579-1593, and vol. XIV, fasc. 5, May 1934, pp. 532-549.
4. Kaplan, Carl: Two-Dimensional Subsonic Compressible Flow past Elliptic Cylinders. NACA Rep. No. 624, 1938.
5. Kaplan, Carl: Compressible Flow about Symmetrical Joukowski Profiles. NACA Rep. No. 621, 1938.
6. Imai, Isao: On the Flow of a Compressible Fluid past a Circular Cylinder. Proc. Phys.-Math. Soc. of Japan, ser. 3, vol. 20, no. 8, Aug. 1938, pp. 636-645.
7. Imai, Isao, and Aihara, Takasi: On the Subsonic Flow of a Compressible Fluid past an Elliptic Cylinder. Rep. No. 194, vol. XV, no. 8, Aero. Res. Inst., Tokyo Imperial Univ., Aug. 1940.
8. Kaplan, Carl: On the Use of Residue Theory for Treating the Subsonic Flow of a Compressible Fluid. NACA Rep. No. 728, 1942.

Method of Small Perturbations

9. Kaplan, Carl: The Flow of a Compressible Fluid past a Curved Surface. NACA Rep. No. 768, 1943.
10. Kaplan, Carl: The Flow of a Compressible Fluid past a Circular Arc Profile. NACA Rep. No. 794, 1944.
11. Kaplan, Carl: Effect of Compressibility at High Subsonic Velocities on the Lifting Force Acting on an Elliptic Cylinder. NACA TN No. 1118, 1946.
12. Kaplan, Carl: Effect of Compressibility at High Subsonic Velocities on the Moment Acting on an Elliptic Cylinder. NACA TN No. 1218, 1947.

13. Hantzsche, W., and Wendt, H.: Der Kompressibilitätseinfluss für dünne wenig gekrümmte Profile bei Unterschallgeschwindigkeit. Z.f.a.M.M., Bd. 22, Nr. 2, April 1942, pp. 72–86. (Available as R.T.P. Translation No. 2198, British Ministry of Aircraft Production.)

Method of the Hodograph

14. Glauert, H.: The Effect of Compressibility on the Lift of an Aerofoil. R. & M. No. 1135, British A.R.C., 1927.

15. Von Kármán, Th.: Compressibility Effects in Aerodynamics. Jour. Aero. Sci., vol. 8, no. 9, July 1941, pp. 337–356.

16. Temple, G., and Yarwood, J.: The Approximate Solution of the Hodograph Equations for Compressible Flow. Rep. No. S.M.E. 3201, British R.A.E., June 1942.

17. Garrick, I. E., and Kaplan, Carl: On the Flow of a Compressible Fluid by the Hodograph Method. I – Unification and Extension of Present-Day Results. NACA Rep No. 789, 1944.

18. Garrick, I. E., and Kaplan, Carl: On the Flow of a Compressible Fluid by the Hodograph Method. II – Fundamental Set of Particular Flow Solutions of the Chaplygin Differential Equation. NACA Rep. No. 790, 1944.

TABLE I.– VALUES OF MAXIMUM VELOCITY FOR CORRESPONDING

BUMP AND CIRCULAR ARC PROFILE

M	q_{max}									
	Camber coefficient, h					Thickness coefficient, t				
	0.02	0.04	0.06	0.08	0.10	0.052	0.100	0.145	0.186	0.226
0	1.0815	1.1659	1.2527	1.3415	1.4320	1.0816	1.1660	1.2527	1.3414	1.4320
.2	1.0834	1.1701	1.2597	1.3520	1.4466	1.0834	1.1701	1.2595	1.3513	1.4454
.3	1.0859	1.1759	1.2695	1.3668	1.4673	1.0859	1.1757	1.2689	1.3651	1.4641
.4	1.0899	1.1851	1.2855	1.3913	1.5024	1.0900	1.1847	1.2840	1.3876	1.4950
.5	1.0960	1.1997	1.3116	1.4324	1.5627	1.0959	1.1988	1.3084	1.4245	1.5467
.6	1.1056	1.2239	1.3572	1.5078	1.6780	1.1052	1.2217	1.3492	1.4879	1.6373
.7	1.1223	1.2705	1.4530	1.6780	------	1.1213	1.2640	1.4298	1.6197	------
.8	1.1594	1.3979	------	------	------	1.1557	1.3701	------	------	------
.9	1.2055	------	------	------	------	1.1960	------	------	------	------

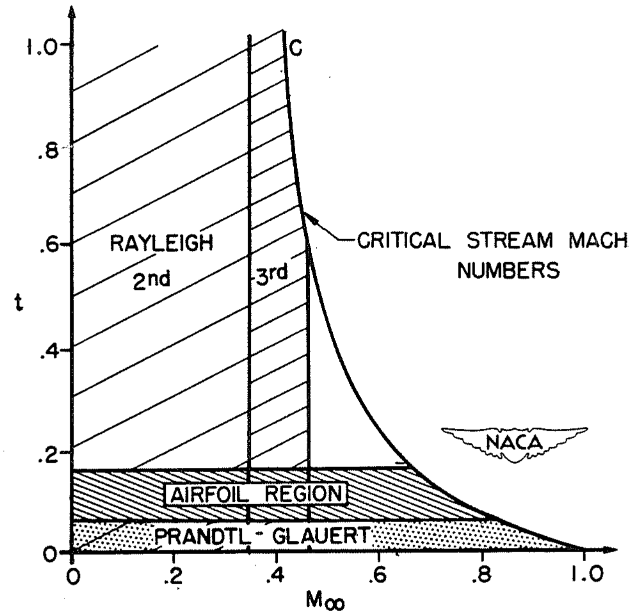

Figure 1.- Regions of application of the approximation methods.

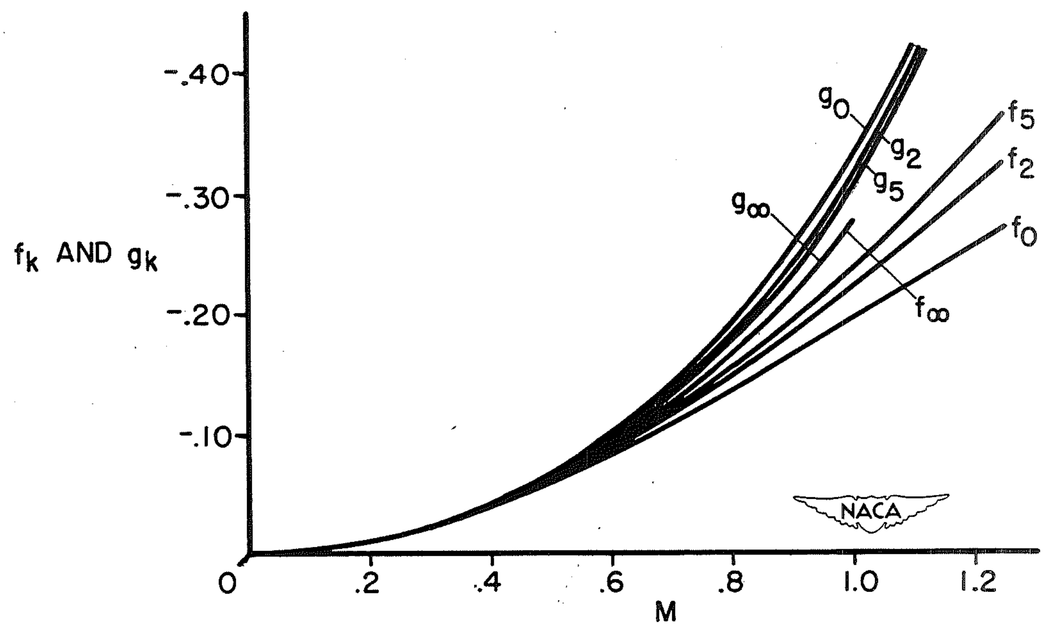

Figure 2.- The f_k and g_k functions against M.

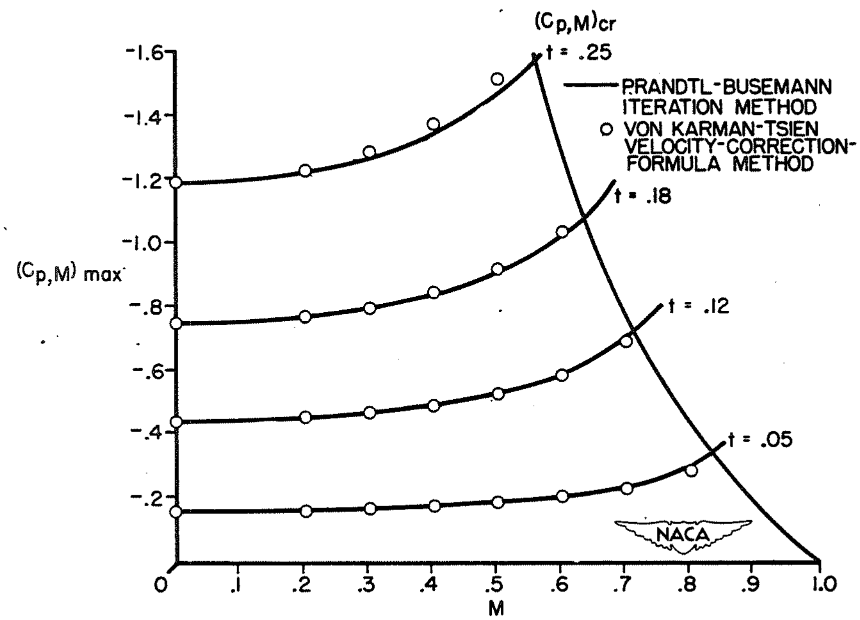

Figure 3.- Maximum pressure coefficient as function of Mach number.